How to cite: *Angew. Chem. Int. Ed.* **2026**, *65*, e16078
doi.org/10.1002/anie.202516078

Photoelectrochemistry

Chiral Gadolinium Halides with Narrow Ultraviolet B Circularly Polarized Luminescence

*Tianyin Shao, Wenkai Zhao, Xinyi Niu, Haolin Lu, Xin Zeng, Hebin Wang, Zhaoyu Wang, Wenting Liu, Bing Sun, Hao-Li Zhang, Yongsheng Chen, and Guankui Long**

Abstract: Circularly polarized luminescence (CPL) in the ultraviolet B (UVB) region holds great potential applications in asymmetric catalysis, enantioselective polymerization, and polarization-based optical anticounterfeiting and information encryption. However, to date, the CPL materials in the UVB region remain unexplored. In this study, the first chiral gadolinium-based organic–inorganic hybrid metal halides, $(R/S\text{-}C_3H_7NF_3)_3GdCl_6$ (***R*/*S*-3F-Gd**), were constructed, which exhibit efficient CPL in the UVB region. Owing to the unique 4*f*-4*f* transition of Gd^{3+} ions, ***R*/*S*-3F-Gd** shows a high photoluminescent quantum yield of 18%, a narrow full width at half maximum (~3 nm) and a ultralong photoluminescence lifetime (~6.6 ms). Additionally, their CPL can be further tuned by applying the external magnetic field. Then the light-emitting diode (LED) chips coated with ***R*-** or ***S*-3F-Gd** were also fabricated, which exhibit high dissymmetry factor of $+ 9.1 \times 10^{-3}$ and -8.2×10^{-3}, further demonstrate their potential as circularly polarized light source in the UVB region. Our work offers a novel strategy for designing the chiral luminescent materials with efficient CPL response in the UVB region and broadens the family of chiral organic–inorganic hybrid rare-earth halides.

Introduction

Circularly polarized light in the ultraviolet B region (UVB) has attracted considerable research interest due to its widespread application prospects in optical information storage or encryption, asymmetric catalysis, and enantioselective polymerization.[1–7] Traditionally, circularly polarized light in the UVB region can be generated through the physical method by using a linear polarizer and a quarter-wave plate, which can lead to half energy losses by the linear polarizer.[8,9] Recently, developing the chiral luminescent materials that can directly emit left- or right-handed circularly polarized luminescence (CPL) has provided a novel strategy for reducing the energy loss and achieving miniaturization of devices.[10,11] However, owing to the band gap limitation, the development of CPL-active materials with efficient UVB-CPL remains unaddressed.

Recent research revealed that chiral organic–inorganic hybrid metal halides (OIHMHs) are one of the best candidates for circularly polarized light sources, owing to their simple synthesis, flexible crystal structure and tunable emission wavelength.[12–21] In the visible light region, chiral OIHMHs with both high photoluminescence quantum yield (PLQY) and large luminescence dissymmetry factor (g_{lum}) have been extensively explored.[22–32] Trivalent rare-earth ions (RE^{3+}) have attracted wide research attention in lighting applications due to their unique electronic configurations, longer luminescence lifetime, narrow emission bandwidth, and coverage of the entire emission spectral region from the ultraviolet to the near-infrared region.[33–36] As shown in Scheme 1, distinct from the broad emission band originating from the *f*-*d* transitions of cerium (III) ions (Ce^{3+}), gadolinium (III) ions (Gd^{3+}) exhibit the characteristic narrow emission band associated with the 4*f*-4*f* electronic transition.[37–39] On the other hand, the unique $4f^7$ electronic configuration of Gd^{3+} gives rise to the lack of low-lying energy levels and the relatively stable $^8S_{7/2}$ ground state, which results in the 4*f*-4*f* electronic transition of Gd^{3+} occurring in the UVB region.[34] Recently, Gd^{3+} has attracted significant attention in the field of magnetic refrigeration and ultraviolet-emitting phosphors.[40–47] Therefore, coupling Gd^{3+} ions with chirality to develop the Gd-based chiral OIHMHs is expected to overcome the inherent bandgap limitations of conventional chiral OIHMHs and realize the efficient CPL response in the UVB region.

[*] T. Shao, W. Zhao, X. Niu, H. Lu, X. Zeng, H. Wang, Z. Wang, W. Liu, Prof. G. Long
Frontiers Science Center for New Organic Matter, Tianjin Key Lab for Rare Earth Materials and Applications, Renewable Energy Conversion and Storage Center (RECAST), School of Materials Science and Engineering, National Institute for Advanced Materials, Nankai University, Tianjin 300350, China
E-mail: longgk09@nankai.edu.cn

Prof. B. Sun, Prof. H.-L. Zhang
State Key Laboratory of Natural Product Chemistry, Key Laboratory of Special Function Materials and Structure Design (MOE), College of Chemistry and Chemical Engineering, Lanzhou University, Lanzhou 730000, China

Prof. Y. Chen
The Centre of Nanoscale Science and Technology and State Key Laboratory of Elemento-Organic Chemistry, Frontiers Science Center for New Organic Matter, College of Chemistry, Nankai University, Tianjin 300350, China

Additional supporting information can be found online in the Supporting Information section

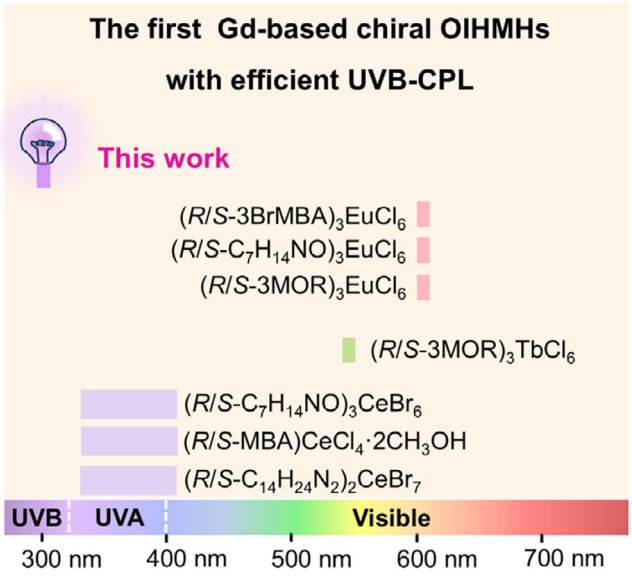

Scheme 1. The first chiral Gd-based OIHMHs with efficient CPL in the UVB region. Comparison between the emission wavelengths and FWHM of chiral rare-earth-based OIHMHs reported in literatures and this work.[32,38,39,48,49]

In this work, we constructed the first Gd-based chiral OIHMHs, $(R/S\text{-}C_3H_7NF_3)_3GdCl_6$ (***R*/*S*-3F-Gd**), and systematically investigated their chiroptical properties. It is found that these chiral Gd-based halides exhibit light emission in the UVB region with a high PLQY of 18%, a narrow full width at half maximum (FWHM) close to 3.03 nm, and long photoluminescence (PL) lifetime estimated to be 6.6 ms. Most importantly, the g_{lum} of ***R*/*S*-3F-Gd** at 312 nm can reach 1.54×10^{-3}, and the figure of merit (FOM = PLQY × $\lfloor g_{lum} \rfloor$) is comparable to other reported chiral OIHMHs. On the other hand, the CPL of ***R*/*S*-3F-Gd** can be further modulated by applying the external magnetic field. Then the light-emitting diode (LED) chips coated with ***R***- or ***S*-3F-Gd** were also fabricated, which exhibit the high dissymmetry factor of $+9.1 \times 10^{-3}$ and -8.2×10^{-3} in the UVB region. Therefore, these chiral gadolinium halides exhibit great potential as the circularly polarized light source in the UVB region, and our work offers a unique strategy to construct the novel UVB-CPL materials and broaden the family of chiral OIHMHs.

Results and Discussion

R/*S*-1,1,1-trifluoropropan-2-amine-hydrochloride are employed to construct the chiral Gd-based OIHMHs. The plate-like crystals were collected and the crystal structures were determined by the single-crystal X-ray diffraction (SCXRD). Both ***R***- and ***S*-3F-Gd** crystallize into the monoclinic system with the *Sohncke* space group of $P2_1$, and the detailed cell parameters are summarized in Table S1. The mirror-symmetric crystal structures and the nearly identical cell parameters further confirm the enantiomeric nature of the obtained chiral Gd-based OIHMHs. As shown in Figure 1, the Gd^{3+} ion coordinates with six Cl^- ions, forming the isolated $[GdCl_6]^{3-}$ octahedra. The distortion of $[GdCl_6]^{3-}$ octahedra can be quantitatively determined by the bond length distortion index (D) and bond angle variance (σ^2), which are summarized in Table S2.[50,51] Compared with the previously reported achiral Gd-based OIHMHs, the octahedral of our chiral gadolinium halides exhibit much larger D and σ^2,[52–54] which further confirms that chirality has been successfully transferred to the inorganic framework through the chiral organic cations.[55,56] The Wilson statistics and cumulative intensity distributions of X-ray reflections also corroborate that ***R*/*S*-3F-Gd** contains the non-centrosymmetric inorganic units (Figures S1 and S2).[51] The Hirshfeld surfaces analysis and corresponding two-dimensional (2D) fingerprint plots of ***R*-3F-Gd** further reveal that strong hydrogen bonding interactions exist between the organic cations and inorganic octahedron (Figure S3). The N-H···Cl interactions are the dominant type, accounting for 82.9% of the total interactions and play a key role in stabilizing the crystal structure.[25,57] The octahedra are isolated by the chiral cations in three directions, forming the typical zero-dimensional (0D) structure. Subsequently, the powder X-ray diffraction (PXRD) was performed, and the simulated and experimental results match very well, which indicates that the prepared ***R***- and ***S*-3F-Gd** powders possess high phase purity (Figure S4). As shown in Figures S5 and S6, the energy dispersive spectroscopy (EDS) mapping confirms the uniform distribution of all elements in ***R***- and ***S*-3F-Gd**. Furthermore, the presence of C, N, F, Cl, and Gd elements was further confirmed by the X-ray photoelectron spectroscopy (XPS). The high-resolution XPS spectra show that Gd $4d_{5/2}$ and Gd $4d_{3/2}$ peaks are located at 143.8 eV and 149.8 eV, which indicates the + 3 valence of the Gd ions in ***R***- and ***S*-3F-Gd** (Figure S7).[58–60] The thermogravimetric analysis (TGA) confirms that ***R***- and ***S*-3F-Gd** exhibit excellent thermal stability with a degradation temperature of 178 °C (Figure S8), which indicates these materials are suitable for device application as discussed below.[32,39,61]

The ultraviolet–visible (UV–vis) absorption and circular dichroism (CD) spectra are then measured and shown in Figures 2a and S9. Both ***R***- and ***S*-3F-Gd** exhibit similar absorption bands, and the *Tauc* plot reveals that the bandgap of ***R*-3F-Gd** is approximately 2.49 eV (Figure S10). As shown in Figure S11, the CD signal of ***R***- and ***S*-3F-Gd** is mirror symmetric, further confirming that the chirality is successfully transferred from the chiral organic cations to the inorganic gadolinium halide skeleton. On the other hand, the vibrational circular dichroism (VCD) was also measured. As shown in Figure 2b, the infrared (IR) spectra of ***R***- and ***S*-3F-Gd** are nearly identical from 1020 to 1340 cm^{-1}, which are associated with the C-N, C-F, and C-C stretching vibration, together with the C-H bending vibration. Meanwhile, the VCD spectra are almost mirror-symmetric, which further supports the enantiomeric nature of ***R***- and ***S*-3F-Gd**.[62,63]

To further investigate the optical and electronic properties of these chiral Gd-based OIHMHs, the spin-polarized electronic band structures, density of states (DOS), the isosurface plots of the wave functions, and the transition dipole moments (TDM) were calculated based on density functional theory

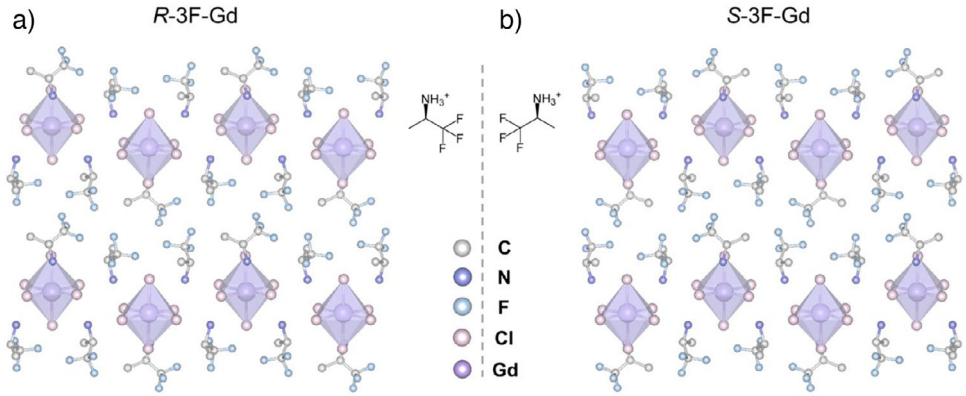

Figure 1. The crystal structures of a) ***R*-3F-Gd** and b) ***S*-3F-Gd**. C, N, F, Cl, and Gd are represented by the light gray, purple, blue, red, and pink spheres, respectively. H atoms are omitted for clarity.

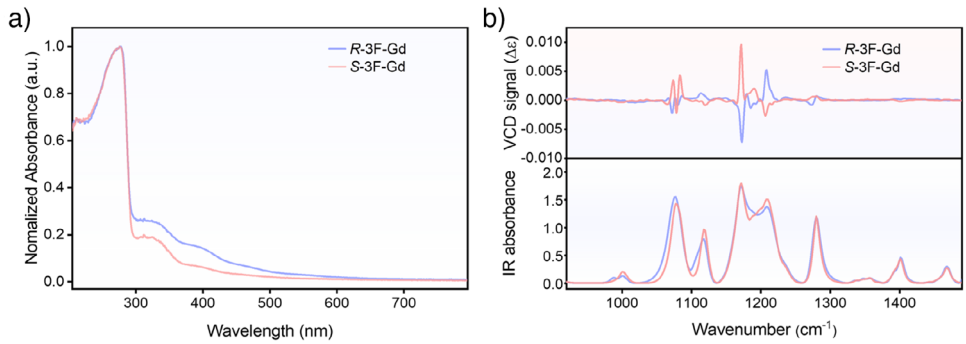

Figure 2. a) The UV–vis absorption spectra of ***R***- and ***S*-3F-Gd**. b) The experimental VCD and IR spectra for ***R***- and ***S*-3F-Gd**.

(DFT). As shown in Figure 3a,b, the flat electronic bands in both the spin-up and spin-down channels are consistent with the typical 0D features of OIHMHs.[64]

In the UV–vis absorption spectrum, there are three absorption peaks, which are labeled as peak 1, 2 and 3. Since peak 1 and 2 are similar in both peak shape and position, they should belong to the same type of electronic transition. Owing to the relatively large ion radius of Gd^{3+}, which results in higher effective nuclear charge that weakens the covalent bond between Gd and Cl. This reduction in covalency leads to weaker hybridization between the Gd 4*f* and Cl 3*p* orbitals, which allows for two distinct transitions: one arises from the electronic transition from Cl 3*p* to Gd 4*f* orbitals, while the other corresponds to the typical *f*-*f* transitions from Gd 4*f* to Gd 4*f* orbitals.[52]

The square of the TDM reflects the transition probability between the valence and conduction bands, with higher value indicating more favorable transitions. As shown in Figures S12–S17, the calculated results show that for the type of Cl 3*p* to Gd 4*f* transition, significant contributions are observed in the spin-up channel for transitions such as 191→206, 199→203, 200→203, 201→204, 201→205, and 202→205, and in the spin-down channel for transitions such as 186→203, 186→204, 186→211, 187→200, 188→193, and 188→205. The excitation energy range for the spin-up transitions matches that of peak 2, whereas the excitation energy range for the spin-down transitions corresponds to peak 1. For the Gd 4*f* to Gd 4*f* transitions, the main contributors in the spin-up channel are transitions such as 159→206, 159→207, 160→203, 160→205, 163→207, and 163→208, with their excitation energy range aligning with peak 3. Furthermore, by plotting the wavefunction isosurface diagrams of these key transitions, the orbital origins of each transition can be visually confirmed. As shown in Figures S15–S17, for peak 1 and 2, the corresponding transitions originate from Cl 3*p* to Gd 4*f* orbitals, whereas for peak 3, the transition occurs from Gd 4*f* to Gd 4*f* orbitals (Figure 3c,d). Overall, the calculated electronic structures are in good agreement with the experimental absorption spectra, which emphasizes the crucial role of the unique $4f^7$ electronic configuration of the Gd(III) ion in determining the optical properties of our chiral OIHMHs.

The excited state dynamics of ***R***- and ***S*-3F-Gd** were then investigated by using the steady-state PL, corresponding PL excitation (PLE) and time-resolved photoluminescence (TRPL) spectra. In the PLE spectra, three peaks centered at 247, 254 and 274 nm are observed, which correspond to the $^8S_{7/2}\rightarrow{}^6D_{7/2}$, $^8S_{7/2}\rightarrow{}^6D_{9/2}$ and $^8S_{7/2}\rightarrow{}^6I_j$ ($j = 7/2, 9/2, 11/2, 13/2, 15/2$, and $17/2$) transitions, respectively (Figure 4a).[44,65–67] Upon excitation at 274 nm, both ***R***- and ***S*-3F-Gd** exhibit the same emission centered at 306 and 312 nm in the UVB region (Figures 4b and S18).[68] The shoulder emission peak is assigned to the $^6P_{5/2}\rightarrow{}^8S_{7/2}$ transition, whereas the strongest

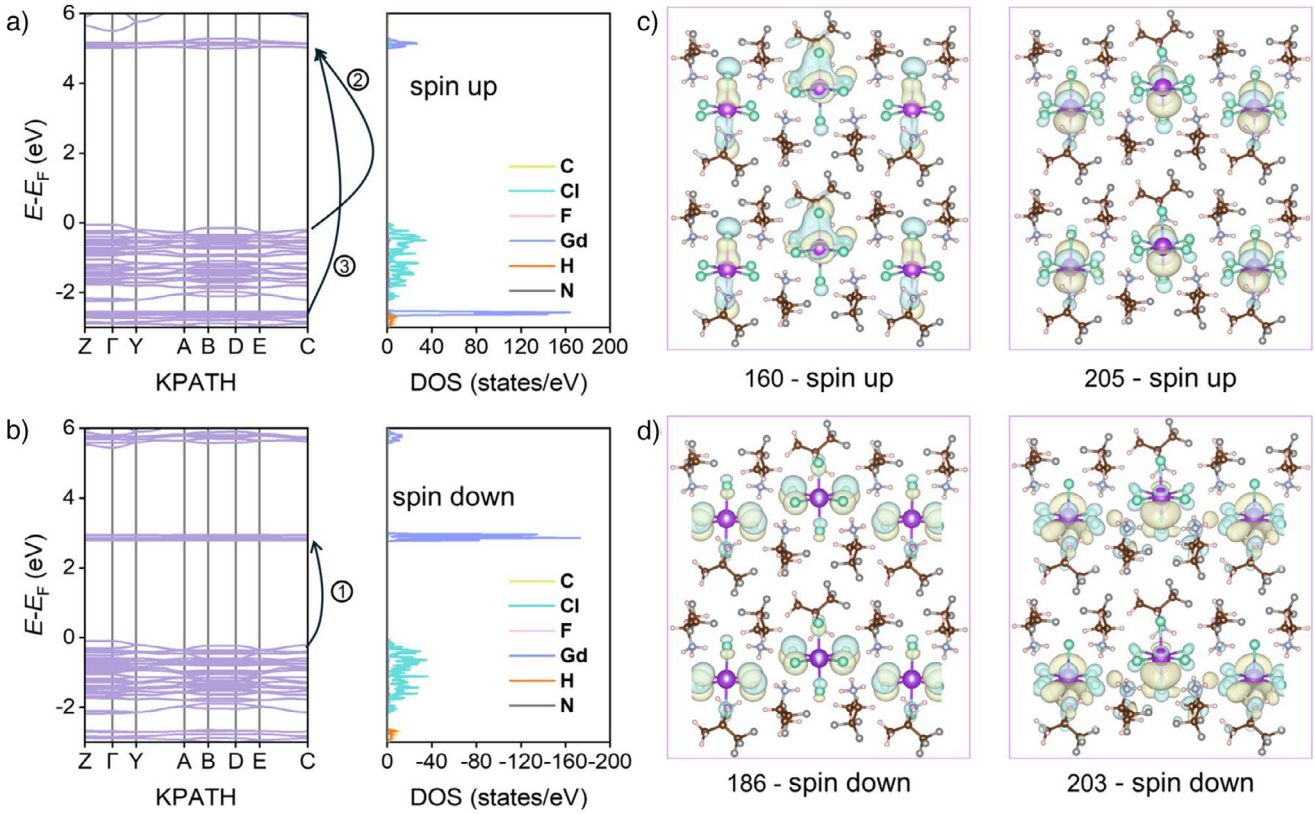

Figure 3. The calculated spin-polarized electronic band structures and partial DOS of ***R*-3F-Gd**, a) spin-up and b) spin-down. The isosurface plots of the wave functions of ***R*-3F-Gd**, c) 160→205 of the spin-up channel and d) 186→203 of the spin-down channel.

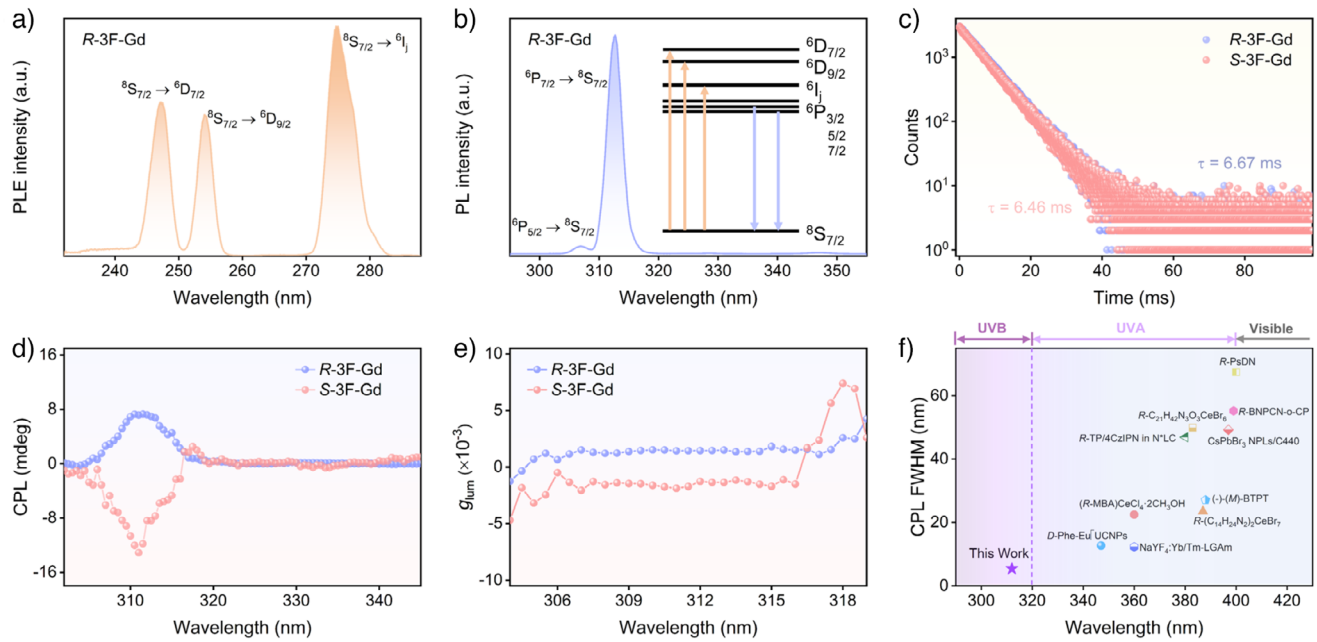

Figure 4. a) The PLE spectra of ***R*-3F-Gd** under emission at 312 nm ($j = 7/2$, 9/2, 11/2, 13/2, 15/2, and 17/2). b) The PL spectra of ***R*-3F-Gd** under excitation at 274 nm. c) The time-resolved PL decay curves of ***R***- and ***S*-3F-Gd** monitored at 312 nm. d) The CPL spectra of ***R***- and ***S*-3F-Gd**. e) The corresponding g_{lum} spectra of ***R***- and ***S*-3F-Gd**. f) Comparison between the emission wavelength and FWHM of the ultraviolet CPL materials reported in literatures and this work.

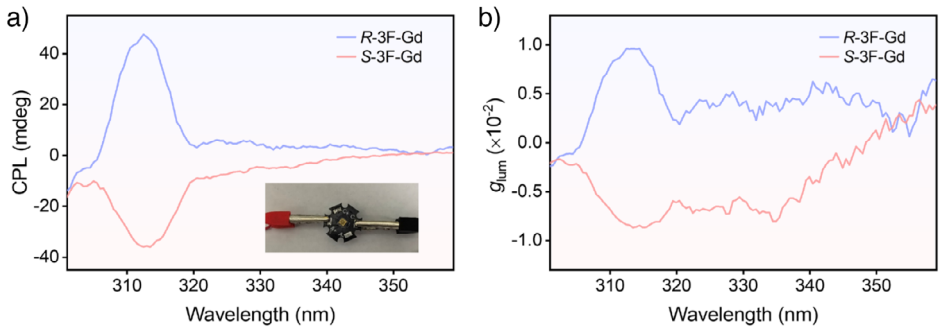

Figure 5. a) The CPL spectra of the LED chips coated with ***R***- and ***S*-3F-Gd**. b) The corresponding g_{lum} spectra of the LED chips coated with ***R***- and ***S*-3F-Gd**. The insets show photographs of the LED chip coated with ***R*-3F-Gd**.

emission peak is attributed to the $^6P_{7/2}\rightarrow{}^8S_{7/2}$ transition of Gd(III) ions. The TRPL spectra are shown in Figure 4c, and the PL lifetime of ***R***- and ***S*-3F-Gd** is estimated to be 6.67 and 6.46 ms, respectively. The longer lifetime at the millisecond level arises from the 4*f*-4*f* Laporte (parity) forbidden transitions,[69] and the FWHM centered at 312 nm is around 3.03 nm at room temperature. The narrow emission is attributed to the quasi-atomic behavior of Gd^{3+} ions benefiting from the shielding effect by the external 5 *s* and 5*p* electrons, which maintain the 4*f*-4*f* electronic transitions undisturbed by the external coordination environment.[34,48] Moreover, the PLQYs of ***R***- and ***S*-3F-Gd** can reach up to 17.70% and 18.24% (λ_{ex} = 274 nm) at room temperature (Figure S19).

To further explore the chiroptical properties, the CPL spectra of ***R***- and ***S*-3F-Gd** are measured upon 274 nm excitation, and shown in Figure 4d. The obvious mirror-symmetric CPL signals are observed from 300 to 320 nm and the CPL peaks are located at 312 nm. To further quantify the dissymmetry of the circularly polarized emission, g_{lum} is calculated by $g_{lum} = 2(I_L - I_R)/(I_L + I_R)$, where I_L and I_R represent the intensities of the left- and right-handed CPL.[70,71] As shown in Figure 4e, the calculated g_{lum} of ***R***- and ***S*-3F-Gd** at 312 nm is $+1.54 \times 10^{-3}$ and -1.33×10^{-3}, respectively. To the best of our knowledge, this is the first report of chiral materials with CPL in the UVB region (Figure 4f).

Moreover, the FOM was also calculated to evaluate the CPL brightness, as defined by Equation (1).[39,72]

$$\text{FOM} = |g_{lum}| \times \text{PLQY} \quad (1)$$

As shown in Table S3, the calculated FOM of ***R***- and ***S*-3F-Gd** are 0.27×10^{-3} and 0.23×10^{-3}, respectively. Compared with the reported FOM in literatures, ***R***- and ***S*-3F-Gd** exhibit comparable FOM but achieve CPL in the UVB region (Figure S20).

The influence of the external magnetic field on the CPL of ***R***- and ***S*-3F-Gd** was also investigated at ± 1.6 T. As shown in Figure S21, the CPL intensity of the $^6P_{7/2}\rightarrow{}^8S_{7/2}$ transition of Gd^{3+} ion in ***R*-3F-Gd** is significantly enhanced under an external magnetic field of −1.6 T, while which is greatly decreased when the magnetic field increases to +1.6 T. For ***S*-3F-Gd**, the influence of external magnetic field is reversed. Moreover, the g_{lum} of ***R*-3F-Gd** can be enhanced by 71% from 1.64×10^{-3} (0 T) to 2.81×10^{-3} (-1.6 T), while which reduced by −69% to 0.51×10^{-3} at +1.6 T (Table S6). Therefore, the CPL response of the $4f - 4f$ transitions in the UVB region can be modulated by the external magnetic field, which is associated with the unique half-filled electron configuration of Gd (III) ions.

Furthermore, the narrow UVB-CPL properties of these chiral gadolinium halides further inspire us to fabricate the circularly polarized LEDs. The ***R***- and ***S*-3F-Gd** powders were dispersed in polymethyl methacrylate (PMMA), which were further spin-coated onto the commercial UV-LED chips (275 nm, 600 mW). Subsequently, the CPL performance of the Gd-based LED was measured and shown in Figure 5a. The mirror-symmetric CPL signals with the prominent peaks at 312 nm were observed, and the calculated g_{lum} of ***R***- and ***S*-3F-Gd** are around $+9.1 \times 10^{-3}$ and -8.2×10^{-3}, respectively (Figure 5b).

Conclusion

In summary, the first chiral gadolinium halides, ***R***- and ***S*-3F-Gd** were designed and constructed to achieve the CPL response in the UVB region unprecedentedly. Structural characterization, CD, VCD and CPL measurements demonstrate that the chirality was successfully transferred from the chiral organic cations to the inorganic gadolinium halide skeleton. ***R***- and ***S*-3F-Gd** exhibit highly efficient CPL in the UVB region with PLQYs of 17.70% and 18.24%, which originates from the 4*f*–4*f* transition of Gd^{3+}. In addition, their CPL signals can be further modulated by applying the external magnetic field. Moreover, the LED chips coated with ***R***- and ***S*-3F-Gd** exhibit efficient UVB-CPL, which further confirms their potential as the circularly polarized light source in the UVB region. Our work offers a unique strategy to achieve the efficient CPL response in the UVB region and broadens the family of chiral organic–inorganic hybrid rare-earth halides.

Acknowledgements

The authors gratefully acknowledge the financial support from the National Natural Science Foundation of China

(52473305, 92256202, U22A20399, 52541104 and 22405111), the Fundamental Research Funds for the Central Universities, Nankai University (grant number: 023-63233038), and the 111 Project (B18030). All the theoretical calculations were performed at the Supercomputing Center of Lanzhou University.

Conflict of Interests

The authors declare no conflict of interest.

Data Availability Statement

The data that support the findings of this study are available in the Supporting Information of this article.

Keywords: Chiral perovskite · Chiral rare-earth halide · Circularly polarized luminescence · *f-f* transition · Ultraviolet B

[1] F. Furlan, J. M. Moreno-Naranjo, N. Gasparini, S. Feldmann, J. Wade, M. J. Fuchter, *Nat. Photon.* **2024**, *18*, 658–668, https://doi.org/10.1038/s41566-024-01408-z.
[2] G. Balavoine, A. Moradpour, H. B. Kagan, *J. Am. Chem. Soc.* **1974**, *96*, 5152–5158, https://doi.org/10.1021/ja00823a023.
[3] T. Kawasaki, M. Sato, S. Ishiguro, T. Saito, Y. Morishita, I. Sato, H. Nishino, Y. Inoue, K. Soai, *J. Am. Chem. Soc.* **2005**, *127*, 3274–3275, https://doi.org/10.1021/ja0422108.
[4] G. Yang, Y. Y. Xu, Z. D. Zhang, L. H. Wang, X. H. He, Q. J. Zhang, C. Y. Hong, G. Zou, *Chem. Comm.* **2017**, *53*, 1735–1738, https://doi.org/10.1039/C6CC09256J.
[5] N. P. M. Huck, W. F. Jager, B. de Lange, B. L. Feringa, *Science* **1996**, *273*, 1686–1688, https://doi.org/10.1126/science.273.5282.1686.
[6] X. Yang, X. Jin, A. Zheng, P. Duan, *ACS Nano* **2023**, *17*, 2661–2668, https://doi.org/10.1021/acsnano.2c10646.
[7] D.-Y. Liu, L.-Y. Xiong, X.-Y. Dong, Z. Han, H.-L. Liu, S.-Q. Zang, *Angew. Chem. Int. Ed.* **2024**, *63*, e202410416, https://doi.org/10.1002/anie.202410416.
[8] Y. Sang, J. Han, T. Zhao, P. Duan, M. Liu, *Adv. Mater.* **2020**, *32*, 1900110, https://doi.org/10.1002/adma.201900110.
[9] Y. Deng, M. Wang, Y. Zhuang, S. Liu, W. Huang, Q. Zhao, *Light Sci. Appl.* **2021**, *10*, 76, https://doi.org/10.1038/s41377-021-00516-7.
[10] J. Li, Q. Luo, J. Wei, L. Zhou, P. Chen, B. Luo, Y. Chen, Q. Pang, J. Z. Zhang, *Angew. Chem. Int. Ed.* **2024**, *63*, e202405310, https://doi.org/10.1002/anie.202405310.
[11] G. Long, R. Sabatini, M. I. Saidaminov, G. Lakhwani, A. Rasmita, X. Liu, E. H. Sargent, W. Gao, *Nat. Rev. Mater.* **2020**, *5*, 423–439, https://doi.org/10.1038/s41578-020-0181-5.
[12] W. Cai, J. Qin, T. Pang, X. Cai, R. Jia, F. Gao, *Adv. Optical Mater.* **2022**, *10*, 2102140, https://doi.org/10.1002/adom.202102140.
[13] Y. Dang, X. Liu, B. Cao, X. Tao, *Matter* **2021**, *4*, 794–820, https://doi.org/10.1016/j.matt.2020.12.018.
[14] J. Ma, H. Wang, D. Li, *Adv. Mater.* **2021**, *33*, 2008785, https://doi.org/10.1002/adma.202008785.
[15] J. Son, G. Jang, S. Ma, H. Lee, C. U. Lee, S. Yang, J. Lee, S. Moon, W. Jeong, J. H. Park, J. Kim, D. H. Kim, J.-S. Park, J. Moon, *Adv. Funct. Mater.* **2025**, *35*, 2413041, https://doi.org/10.1002/adfm.202413041.
[16] L. Wang, Y. Xue, M. Cui, Y. Huang, H. Xu, C. Qin, J. Yang, H. Dai, M. Yuan, *Angew. Chem. Int. Ed.* **2020**, *132*, 6504–6512, https://doi.org/10.1002/ange.201915912.
[17] G. Long, C. Jiang, R. Sabatini, Z. Yang, M. Wei, L. N. Quan, Q. Liang, A. Rasmita, M. Askerka, G. Walters, X. Gong, J. Xing, X. Wen, R. Quintero-Bermudez, H. Yuan, G. Xing, X. R. Wang, D. Song, O. Voznyy, M. Zhang, S. Hoogland, W. Gao, Q. Xiong, E. H. Sargent, *Nat. Photon.* **2018**, *12*, 528–533, https://doi.org/10.1038/s41566-018-0220-6.
[18] D. Fu, J. Xin, Y. He, S. Wu, X. Zhang, X. M. Zhang, J. Luo, *Angew. Chem. Int. Ed.* **2021**, *60*, 20021–20026, https://doi.org/10.1002/anie.202108171.
[19] H. Lu, J. Wang, C. Xiao, X. Pan, X. Chen, R. Brunecky, J. J. Berry, K. Zhu, M. C. Beard, Z. V. Vardeny, *Sci. Adv.* **2019**, *5*, eaay0571, https://doi.org/10.1126/sciadv.aay0571.
[20] H. Zheng, A. Ghosh, M. J. Swamynadhan, Q. Zhang, W. P. D. Wong, Z. Wu, R. Zhang, J. Chen, F. Cimpoesu, S. Ghosh, B. J. Campbell, K. Wang, A. Stroppa, R. Mahendiran, K. P. Loh, *Nat. Commun.* **2024**, *15*, 5556, https://doi.org/10.1038/s41467-024-49708-w.
[21] G. Chen, X. Liu, J. An, S. Wang, X. Zhao, Z. Gu, C. Yuan, X. Xu, J. Bao, H.-S. Hu, J. Li, X. Wang, *Nat. Chem.* **2023**, *15*, 1581–1590, https://doi.org/10.1038/s41557-023-01290-2.
[22] J. Chen, S. Zhang, X. Pan, R. Li, S. Ye, A. K. Cheetham, L. Mao, *Angew. Chem. Int. Ed.* **2022**, *61*, e202205906, https://doi.org/10.1002/anie.202205906.
[23] L. Du, Q. Zhou, Q. He, Y. Liu, Y. Shen, H. Lv, L. Sheng, T. Cheng, H. Yang, L. Wan, Y. Fang, W. Ning, *Adv. Funct. Mater.* **2024**, *34*, 2315676, https://doi.org/10.1002/adfm.202315676.
[24] J.-X. Gao, W.-Y. Zhang, Z.-G. Wu, Y.-X. Zheng, D.-W. Fu, *J. Am. Chem. Soc.* **2020**, *142*, 4756–4761, https://doi.org/10.1021/jacs.9b13291.
[25] X. Han, P. Cheng, H. Yang, J. Guan, M. Xin, G. Li, X. Li, Y. Zheng, J. Xu, X. H. Bu, *Angew. Chem. Int. Ed.* **2025**, *64*, e202419776, https://doi.org/10.1002/anie.202419776.
[26] M. Li, Y. Wang, L. Yang, Z. Chai, Y. Wang, S. Wang, *Angew. Chem. Int. Ed.* **2022**, *61*, e202208440, https://doi.org/10.1002/anie.202208440.
[27] D. Y. Liu, H. Y. Li, R. P. Han, H. L. Liu, S. Q. Zang, *Angew. Chem. Int. Ed.* **2023**, *62*, e202307875, https://doi.org/10.1002/anie.202307875.
[28] C.-M. Shi, H. Lu, J.-Y. Wang, G. Long, L.-J. Xu, Z.-N. Chen, *Nat. Commun.* **2025**, *16*, 1505, https://doi.org/10.1038/s41467-025-56394-9.
[29] T. Song, C. Q. Wang, H. Lu, X. J. Mu, B. L. Wang, J. Z. Liu, B. Ma, J. Cao, C. X. Sheng, G. Long, Q. Wang, H. L. Zhang, *Angew. Chem. Int. Ed.* **2024**, *63*, e202400769, https://doi.org/10.1002/anie.202400769.
[30] H. L. Xuan, J. L. Li, L. J. Xu, D. S. Zheng, Z. N. Chen, *Adv. Optical Mater.* **2022**, *10*, 2200591, https://doi.org/10.1002/adom.202200591.
[31] L. Yao, G. Niu, J. Li, L. Gao, X. Luo, B. Xia, Y. Liu, P. Du, D. Li, C. Chen, Y. Zheng, Z. Xiao, J. Tang, *J. Phys. Chem. Lett.* **2020**, *11*, 1255–1260, https://doi.org/10.1021/acs.jpclett.9b03478.
[32] Y. Zhang, Y. Wei, C. Li, Y. Wang, Y. Liu, M. He, Z. Luo, X. Chang, X. Kuang, Z. Quan, *Chem. Commun.* **2025**, *61*, 85–88, https://doi.org/10.1039/D4CC05206D.
[33] Y. Zhong, Z. Wu, Y. Zhang, B. Dong, X. Bai, *InfoMat.* **2023**, *5*, e12392, https://doi.org/10.1002/inf2.12392.
[34] B. Zheng, J. Fan, B. Chen, X. Qin, J. Wang, F. Wang, R. Deng, X. Liu, *Chem. Rev.* **2022**, *122*, 5519–5603, https://doi.org/10.1021/acs.chemrev.1c00644.
[35] Y. Zhang, S. Yu, B. Han, Y. Zhou, X. Zhang, X. Gao, Z. Tang, *Matter* **2022**, *5*, 837–875, https://doi.org/10.1016/j.matt.2022.01.001.

[36] X. Zhou, L. Ning, J. Qiao, Y. Zhao, P. Xiong, Z. Xia, *Nat. Commun.* **2022**, *13*, 7589, https://doi.org/10.1038/s41467-022-35366-3.
[37] Q. Wang, T. Bai, S. Ji, H. Zhao, X. Meng, R. Zhang, J. Jiang, F. Liu, *Adv. Funct. Mater.* **2023**, *33*, 2303399, https://doi.org/10.1002/adfm.202303399.
[38] X. Niu, Z. Zeng, Z. Wang, H. Lu, B. Sun, H.-L. Zhang, Y. Chen, Y. Du, G. Long, *Sci. China Chem.* **2024**, *67*, 1961–1968, https://doi.org/10.1007/s11426-024-1946-7.
[39] C. Li, Y. Wei, Y. Zhang, Z. Luo, Y. Liu, M. He, Z. Quan, *Angew. Chem. Int. Ed.* **2024**, *63*, e202403727, https://doi.org/10.1002/anie.202403727.
[40] F. Wang, R. Deng, X. Liu, *Nat. Protoc.* **2014**, *9*, 1634–1644, https://doi.org/10.1038/nprot.2014.111.
[41] Y. Liu, D. Tu, H. Zhu, R. Li, W. Luo, X. Chen, *Adv. Mater.* **2010**, *22*, 3266–3271, https://doi.org/10.1002/adma.201000128.
[42] S. Dhale, N. S. Ugemuge, V. Singh, M. S. Shekhawat, S. V. Moharil, *Opt. Mater.* **2024**, *148*, 114888, https://doi.org/10.1016/j.optmat.2024.114888.
[43] X.-Y. Zheng, X.-J. Kong, Z. Zheng, L.-S. Long, L.-S. Zheng, *Acc. Chem. Res.* **2018**, *51*, 517–525, https://doi.org/10.1021/acs.accounts.7b00579.
[44] V. Singh, G. Sivaramaiah, J. L. Rao, S. H. Kim, *J. Lumin.* **2013**, *143*, 162–168, https://doi.org/10.1016/j.jlumin.2013.03.054.
[45] X.-T. Wang, S.-R. He, F.-W. Lv, X.-T. Wang, M.-X. Hong, L. Cao, G.-L. Zhuang, C. Chen, J. Zheng, L.-S. Long, X.-Y. Zheng, *Angew. Chem. Int. Ed.* **2024**, *63*, e202410414, https://doi.org/10.1002/anie.202410414.
[46] Q. Xu, B. Liu, M. Ye, G. Zhuang, L. Long, L. Zheng, *J. Am. Chem. Soc.* **2022**, *144*, 13787–13793, https://doi.org/10.1021/jacs.2c04840.
[47] X. Y. Zheng, H. Zhang, Z. Wang, P. Liu, M. H. Du, Y. Z. Han, R. J. Wei, Z. W. Ouyang, X. J. Kong, G. L. Zhuang, L. S. Long, L. S. Zheng, *Angew. Chem. Int. Ed.* **2017**, *56*, 11475–11479, https://doi.org/10.1002/anie.201705697.
[48] X. Niu, Y. Li, H. Lu, Z. Wang, Y. Zhang, T. Shao, H. Wang, S. Gull, B. Sun, H.-L. Zhang, Y. Chen, K. Wang, Y. Du, G. Long, *Nat. Commun.* **2025**, *16*, 2525, https://doi.org/10.1038/s41467-025-57620-0.
[49] C. Chen, J. Chen, Z. Chen, H. Liu, Z. Zhang, R. Chen, H. Lu, L. Mao, *Inorg. Chem.* **2024**, *63*, 21801–21805, https://doi.org/10.1021/acs.inorgchem.4c03570.
[50] H. Wang, J. Li, H. Lu, S. Gull, T. Shao, Y. Zhang, T. He, Y. Chen, T. He, G. Long, *Angew. Chem. Int. Ed.* **2023**, *62*, e202309600, https://doi.org/10.1002/anie.202309600.
[51] M. K. Jana, R. Song, H. Liu, D. R. Khanal, S. M. Janke, R. Zhao, C. Liu, Z. Valy Vardeny, V. Blum, D. B. Mitzi, *Nat. Commun.* **2020**, *11*, 4699, https://doi.org/10.1038/s41467-020-18485-7.
[52] M. W. Löble, J. M. Keith, A. B. Altman, S. C. E. Stieber, E. R. Batista, K. S. Boland, S. D. Conradson, D. L. Clark, J. L. Pacheco, S. A. Kozimor, R. L. Martin, S. G. Minasian, A. C. Olson, B. L. Scott, D. K. Shuh, T. Tyliszczak, M. P. Wilkerson, R. A. Zehnder, *J. Am. Chem. Soc.* **2015**, *137*, 2506–2523.
[53] R. D. Rogers, A. N. Rollins, R. D. Etzenhouser, E. J. Voss, C. B. Bauer, *Inorg. Chem.* **1993**, *32*, 3451–3462, https://doi.org/10.1021/ic00068a013.
[54] C. C. Hines, D. B. Cordes, S. T. Griffin, S. I. Watts, V. A. Cocalia, R. D. Rogers, *New J. Chem.* **2008**, *32*, 872, https://doi.org/10.1039/b800045j.
[55] Y. Fu, S. Jin, X. Y. Zhu, *Nat. Rev. Chem.* **2021**, *5*, 838–852, https://doi.org/10.1038/s41570-021-00335-9.
[56] S. Gull, W. Zhao, Z. Wang, Y. Zhang, H. Lu, X. Niu, T. Qiao, H. Wang, T. Shao, W. Liu, B. Sun, H. L. Zhang, Y. Chen, G. Long, *Angew. Chem. Int. Ed.* **2025**, *64*, e202502029, https://doi.org/10.1002/anie.202502029.
[57] J. Bai, H. Wang, J. Ma, Y. Zhao, H. Lu, Y. Zhang, S. Gull, T. Qiao, W. Qin, Y. Chen, L. Jiang, G. Long, Y. Wu, *J. Am. Chem. Soc.* **2024**, *146*, 18771–18780, https://doi.org/10.1021/jacs.4c06822.
[58] Y. Liu, L. Zhang, Q. Xu, S. Zhang, Y. Zhou, G. Hu, *Adv. Funct. Mater.* **2025**, *35*, 2413134, https://doi.org/10.1002/adfm.202413134.
[59] A. F. Zatsepin, Y. A. Kuznetsova, D. A. Zatsepin, C.-H. Wong, W.-C. Law, C.-Y. Tang, N. V. Gavrilov, D. V. Boukhwalov, *J. Alloys Compd.* **2023**, *949*, 169815, https://doi.org/10.1016/j.jallcom.2023.169815.
[60] T. Hou, R. Yang, J. Xu, X. He, H. Yang, P. W. Menezes, Z. Chen, *Nanoscale* **2024**, *16*, 15629–15639, https://doi.org/10.1039/D4NR01743A.
[61] T.-H. Yang, H.-Y. Huang, C.-C. Sun, B. Glorieux, X.-H. Lee, Y.-W. Yu, T.-Y. Chung, *Sci. Rep.* **2018**, *8*, 296, https://doi.org/10.1038/s41598-017-18686-z.
[62] C. Shi, L. Ye, Z.-X. Gong, J.-J. Ma, Q.-W. Wang, J.-Y. Jiang, M.-M. Hua, C.-F. Wang, H. Yu, Y. Zhang, H.-Y. Ye, *J. Am. Chem. Soc.* **2020**, *142*, 545–551, https://doi.org/10.1021/jacs.9b11697.
[63] H. Peng, Y. Qin, X. G. Chen, X. J. Song, R. G. Xiong, W. Q. Liao, *Angew. Chem. Int. Ed.* **2025**, *64*, e202500285, https://doi.org/10.1002/anie.202500285.
[64] Z. Guo, J. Li, J. Liang, C. Wang, X. Zhu, T. He, *Nano Lett.* **2022**, *22*, 846–852, https://doi.org/10.1021/acs.nanolett.1c04669.
[65] S. Zhao, S. Kanwal, W. Su, H. Lin, Z. Han, S. Zhuang, D. Yu, D. Zhang, *Opt. Mater.* **2024**, *151*, 115408, https://doi.org/10.1016/j.optmat.2024.115408.
[66] D. He, C. Yu, J. Cheng, S. Li, L. Hu, *J. Rare Earths* **2011**, *29*, 48–51, https://doi.org/10.1016/S1002-0721(10)60392-4.
[67] K. Binnemans, C. Görller-Walrand, J. L. Adam, *Chem. Phys. Lett.* **1997**, *280*, 333–338, https://doi.org/10.1016/S0009-2614(97)01126-3.
[68] X. Yang, D. Chen, Y. Liang, S. Zhou, J. Xu, L. Liu, H. Lin, Y. Xiong, Y. Cheng, Y. Wang, *J. Mater. Chem. C* **2023**, *11*, 6912–6919, https://doi.org/10.1039/D3TC00722G.
[69] H.-Y. Wong, W.-S. Lo, K.-H. Yim, G.-L. Law, *Chem.* **2019**, *5*, 3058–3095, https://doi.org/10.1016/j.chempr.2019.08.006.
[70] T. Zhao, J. Han, P. Duan, M. Liu, *Acc. Chem. Res.* **2020**, *53*, 1279–1292, https://doi.org/10.1021/acs.accounts.0c00112.
[71] Q. Wei, Z. Ning, *ACS Mater. Lett.* **2021**, *3*, 1266–1275, https://doi.org/10.1021/acsmaterialslett.1c00274.
[72] Y. Deng, M. Wang, Y. Zhuang, S. Liu, W. Huang, Q. Zhao, *Light Sci. Appl.* **2021**, *10*, 76, https://doi.org/10.1038/s41377-021-00516-7.

Manuscript received: July 22, 2025
Revised manuscript received: October 21, 2025
Manuscript accepted: December 11, 2025
Version of record online: December 19, 2025